SEISMIC WAVE ATTENUATION AT FULL WATER SATURATION

JACK DVORKIN; Rock Solid Images and Stanford University
GARY MAVKO; Stanford University
JOEL WALLS; Rock Solid Images

SUMMARY

In fully-saturated rock and at ultrasonic frequencies, the microscopic squirt flow induced between the stiff and soft parts of the pore space by an elastic wave is responsible for velocity-frequency dispersion and attenuation. In the seismic frequency range, it is the macroscopic cross-flow between the stiffer and softer parts of the rock. We use the latter hypothesis to introduce simple approximate equations for velocity-frequency dispersion and attenuation in a fully water saturated reservoir. The equations are based on the assumption that in heterogeneous rock and at a very low frequency, the effective elastic modulus of the fully-saturated rock can be estimated by applying a fluid substitution procedure to the averaged (upscaled) dry frame whose effective porosity is the mean porosity and the effective elastic modulus is the Backus-average (geometric mean) of the individual dry-frame elastic moduli of parts of the rock. At a higher frequency, the effective elastic modulus of the saturated rock is the Backus-average of the individual fully-saturated-rock elastic moduli of parts of the rock. The difference between the effective elastic modulus calculated separately by these two methods determines the velocity-frequency dispersion. The corresponding attenuation is calculated from this dispersion by using (e.g.) the standard linear solid attenuation model.

UPPER AND LOWER ELASTIC LIMITS AT FULL SATURATION

Let us assume that a heterogeneous domain of rock includes a number of homogeneous parts with porosity f and the dry-frame compressional modulus M_{Dry} that vary among those parts but are constant within each individual part. Then the effective porosity f_{Eff} of the domain is the arithmetic average of individual porosities:

$$f_{Eff} = \langle f \rangle, \tag{1}$$

and the effective dry-frame compressional modulus is the Backus (geometric) average of individual moduli:

$$M_{DryEff} = \langle M_{Dry}^{-1} \rangle^{-1}. \tag{2}$$

At a very low frequency and in saturated rock, the wave-induced pressure increments equilibrate between the individual parts. As a result, the effective saturated-rock compressional modulus can be calculated by applying the P-only fluid substitution equation (Mavko et al., 1995) to the entire domain under examination:

$$M_{SatEff0} = M_S \frac{f_{Eff} M_{DryEff} - (1 + f_{Eff}) K_F M_{DryEff} / M_S + K_F}{(1 - f_{Eff}) K_F + f_{Eff} M_S - K_F M_{DryEff} / M_S}, \tag{3}$$

where M_S is the mineral-phase compressional modulus, assumed the same for all individual parts of the rock; and is the bulk modulus of the pore fluid, also the same throughout the heterogeneous domain.

At a higher frequency, the individual parts of the domain are undrained. The saturated-rock compressional moduli of each individual part can be calculated by applying the P-only fluid substitution equation individually. Then the effective saturated-rock compressional modulus is the Backus average of the individual saturated-rock compressional moduli:

$$M_{SatEff\infty} = \left\langle \left(M_S \frac{f M_{Dry} - (1 + f) K_F M_{Dry} / M_S + K_F}{(1 - f) K_F + f M_S - K_F M_{Dry} / M_S} \right)^{-1} \right\rangle^{-1}. \tag{4}$$

Consider an example where the heterogeneous domain includes two clean-sand individual parts of equal volumes. The porosities of the two parts are 0.35 and 0.30, the respective dry-frame P-wave velocities are and 2.3 km/s and 2.9 km/s, and the respective dry-frame compressional moduli are 9.11 GPa and 15.6 GPa. The compressional modulus of the solid phase (quartz) is 100 GPa and the bulk modulus of the pore fluid (brine) is 2.7 GPa.

The effective porosity, according to Equation (1), is 0.325 and the effective dry-frame compressional modulus, according to Equation (2), is 11.5 GPa. The corresponding low-frequency saturated-rock compressional modulus $M_{SatEff0}$ is, according to Equation (3), 17.7 GPa.

The individual saturated-rock compressional moduli of the parts of the rock are 15.2 GPa and 21.7 GPa for porosity 0.35 and 0.3, respectively. Then the corresponding highfrequency saturated-rock compressional modulus $M_{SatEff\infty}$ is, according to Equation (4), 17.9 GPa.

The corresponding maximum inverse quality factor, according to the standard linear solid model,

$$(\frac{1}{Q})_{\max} = \frac{M_\infty - M_0}{2\sqrt{M_0 M_\infty}}, \qquad (5)$$

is 0.0056.

INVERSE QUALITY FACTOR FROM WELL LOG DATA

Exactly the same approach can be used if well log data are available. First, the dry-frame compressional modulus is calculated from the original log data as

$$M_{Dry} = M_S \frac{1-(1-f)M_{Sat}/M_S - fM_{Sat}/K_F}{1+f-fM_S/K_F - M_{Sat}/M_S}, \quad (6)$$

where is the product of the measured bulk density and the P-wave velocity squared.

Then the above-described operation is applied to calculate $M_{SatEff0}$, $M_{SatEff\infty}$, and the maximum inverse quality factor. The averaging required can be done along a moving window of a desired length, corresponding, e.g., to a quarter-wavelength.

An example of such calculation is given in Figure 1 for a 1-km-long shaley interval. The resulting inverse quality factor appears to lie within a reasonable range between 0.01 and 0.02 which corresponds to the quality factor Q between 50 and 100.

EFFECT OF SAMPLING IN WELL LOG DATA

An important issue is the stability of the proposed attenuation calculation method with respect to the sampling interval in well log curves. To address this issue we subsampled the original well log data used in Figure 1, whose sampling is a half-foot, with (a) a one-foot interval, and (b) a two-foot interval.

The resulting inverse quality factor is plotted versus depth in the fifth frame of Figure 1. It is essentially identical to that computed from the data with the original (half-foot) sampling rate.

COMPARISON TO AN EMPIRICAL MODEL

The Koesoemadinata and McMechan (2001) model (KOM) is simply a statistical regression to most of the available attenuation data. Unfortunately, no data are available in the seismic frequency range which makes this regression no more than a guess at seismic frequency. Nevertheless, we compare our modeling results to those predicted by KOM, the latter applied to the well log data shown in Figure 1 and assuming constant (50%) clay content and 30 Hz frequency. The KOM inverse quality factor (Figure 1, fifth frame) is larger than that predicted by our model. Still, both curves lie in the same range which indirectly indicates the relevance of the rational model introduced here.

CONCLUSION

Attenuation remains an elusive propagational seismic attribute that is hard to measure and theoretically model. This paper presents an attempt to model attenuation in fully saturated rock using a simple theoretical approach and first physical principles. The main purpose of modeling is not just to predict attenuation but to establish what can be said about the reservoir properties from attenuation. In other words, our aspiration is to make attenuation a reservoir characterization tool. The present work implies that in fully-saturated rock, attenuation is a measure of elastic heterogeneity.

The model introduced here has to be validated by real data which only can come from attenuation calculated from well logs or seismic data.

REFERENCES

Backus, G.F., 1962, Long-wave elastic anisotropy produced by horizontal layering, J. Geophys. Res., 67, 4427-4441.

Koesoemadinata, A.P, and McMechan, G.A., 2001, Empirical estimation of viscoelastic seismic parameters from petrophysical properties of sandstone, Geophysics, 66, 1457-1470.

Mavko, G., Chan, C., and Mukerji, T., 1995, Fluid substitution: Estimating changes in Vp without knowing Vs, Geophysics, 60, 1750-1755.

ACKNOWLEDGEMENT

This work is supported by the RSI Q and Attenuation Project. We gratefully thank these sponsors for their support. The industrial sponsors of this project are;
AGIP, Anadarko, BG Group, Burlington Resources, Enterprise Plc., Marathon, Devon Energy, Norsk Hydro, Saudi Aramco, RWE-DEA, TotalFinaElf, Odegaard AS.

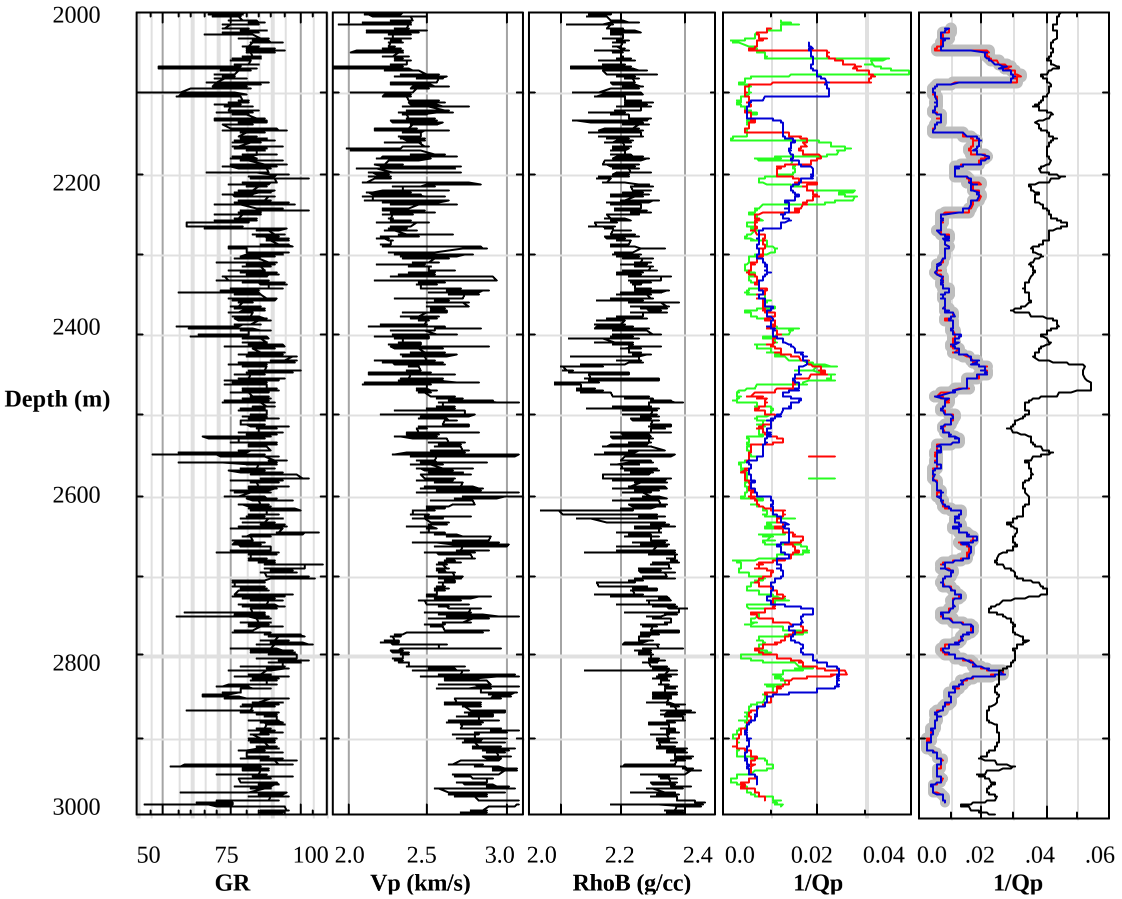

Figure 1. First three frames -- well log data from a water-saturated interval (gamma ray, P-wave velocity, and bulk density). Fourth frame -- calculated inverse P-wave quality factor for three sizes of running window - 75, 38, and 19 m. Fifth frame -- inverse P-wave quality factor calculated from undersampled well log data (red and blue) superimposed on the curve calculated from the original data with the 38 m running window (bold gray curve). Also, in the same frame the black curve is the inverse P-wave quality factor from the Koesoemadinata and McMechan (2001) empirical model, labeled KOM.